Available online at www.sciencedirect.com
SCIENCE DIRECT®
Journal of Molecular Catalysis A: Chemical 222 (2004) 199–205
JOURNAL OF MOLECULAR CATALYSIS A: CHEMICAL
www.elsevier.com/locate/molcata

Enantio-differentiating hydrogenation of methyl acetoacetate over tartaric acid-modified nickel catalysts: effects of preparation method of supported nickel on activity and selectivity of catalysts

Donghyun Jo, Jae Sung Lee, Kyung Hee Lee*

Department of Chemical Engineering, Pohang University of Science and Technology (POSTECH), San 31, Hyoja-Dong, Pohang 790-784, Republic of Korea

Received 7 June 2004; received in revised form 2 August 2004; accepted 4 August 2004
Available online 11 September 2004

Abstract

Enantio-differentiating hydrogenation of methyl acetoacetate was carried out over supported nickel catalysts modified by (*R*,*R*)-tartaric acid and NaBr. The types of support and the preparation methods affected the enantiomeric excess of the obtained product, methyl (*R*)-3-hydroxybutyrate. Nickel supported on aluminum oxide gave the best enantio-selectivity. Silica-supported catalysts showed lower selectivities. In particular, precipitation deposition of nickel on silica forms nickel silicate, which was difficult to be reduced and constituted a lattice defect of nickel surface. Even reduced nickel surface could be contaminated by silicon in nickel silicate. This defect and the surface contamination may disrupt the arranged adsorption of tartaric acid and reduce the enantio-selectivity of the catalysts.

Keywords: Enantio-differentiating hydrogenation; Nickel; Precipitation; Tartaric acid; Methyl acetoacetate

1. Introduction

Supported nickel catalysts are very important in industrial processes. They are easy to handle, highly active, and economic [1,2]. The general methods for the preparation of supported nickel are impregnation, ion-exchange, and precipitation deposition of nickel precursor on the oxide supports [3]. These methods produce different states of nickel on supports that lead to different activity, selectivity, and stability of catalysts.

Tartaric acid-modified nickel is a peculiar heterogeneous catalyst for the enantio-differentiating hydrogenation of β-keto-ester such as methyl acetoacetate [4–9]. It was reported that the dispersion of nickel was a very important factor in this reaction, and modification conditions such as modification time, temperature, pH, the amounts of modifier and co-modifier affected the optical yield of product [10–13]. Generally a large crystallite size of nickel shows a higher optical yield of product [14–16], so the supported nickel catalysts for enantio-differentiating hydrogenation are prepared with high loadings above 40 wt.% for the formation of large nickel crystallites on support. The interaction of nickel with support and the state of nickel on support depend very much on support type and the method of nickel loading [17]. Thus the optical yield of methyl (*R*)-3-hydroxybutyrate, a product of enantio-differentiating hydrogenation of methyl acetoacetate, could also be affected by the type of support and the method of nickel loading.

Catalysts for the enantio-differentiating hydrogenation of methyl acetoacetate have been prepared by the method of homogeneous precipitation deposition in Na_2CO_3 or NH_4OH solution [18–23] and impregnation of supports with a nickel precursor [24–27]. The purpose of this research is to study the effects of preparation method of supported

* Corresponding author. Tel.: +82 54 279 2263/8272; fax: +82 54 279 5528.
E-mail address: kyunglee@postech.ac.kr (K.H. Lee).

1381-1169/$ – see front matter © 2004 Elsevier B.V. All rights reserved.
doi:10.1016/j.molcata.2004.08.001

nickel on the activity and selectivity of the catalyst modified by tartaric acid and sodium bromide solution in the enantio-differentiating hydrogenation of methyl acetoacetate. Impregnation and homogeneous precipitation deposition methods were applied to the preparation of supported nickel, and aluminum oxide and silica were used as supports.

2. Experimental

2.1. Catalyst preparation

Supported nickel catalysts on aluminum oxide (activated, acidic, specific surface area 160.0 m^2/g, Aldrich) or silica (fumed, specific surface area 204.2 m^2/g, Aldrich) were prepared by the impregnation (Imp) and the precipitation deposition (Pre) methods. The weight ratio of nickel to support was 2:3 (40 wt.% nickel loading). Impregnated samples were prepared by the evaporation of water from an aqueous $Ni(NO_3)_2$ (flake, Aldrich) solution containing support powders. Precipitated samples were prepared by the use of sodium carbonate as precipitant at a temperature of 75 °C. The precipitated samples were filtered and washed three times with 500 ml of warm distilled water. These impregnated and precipitated samples were dried at 100 °C for 12 h, calcined at 500 °C for 5 h under static air atmosphere, and then finally reduced at 500 °C for 2 h in a hydrogen flow of 2.0 mmol/min.

The reduced sample was modified by an aqueous (*R*,*R*)-tartaric acid (99%, natural tartaric acid, Aldrich) and sodium bromide solution. Under inert atmosphere, 6.7 mmol of (*R*,*R*)-tartaric acid was mixed with 100 ml distilled water. The pH of modification solution was controlled to 2.5 by adding a 1N NaOH solution. With vigorous stirring, the modification solution was degassed under vacuum. The reduced catalyst was immersed in the modification solution at 50 °C for 40 min. The co-modifier, sodium bromide (48.6 mmol) was then added and the modification was continued at an increased temperature of 100 °C for 20 min. The modified catalyst was separated from the modification solution by centrifuge and washed two times with methanol.

2.2. Enantio-differentiating hydrogenation of methyl acetoacetate

A stainless steel autoclave (50 ml, Autoclave Engineers Inc.) with a magnetic stirrer was used for high pressure reactions. With 5 g of methanol solvent, 43.1 mmol of methyl acetoacetate (99%, Acros) was hydrogenated over 0.6 g of modified nickel catalyst at 100 °C. The pressure of hydrogen was initially 9.0 MPa and decreased as reaction progressed.

In order to calculate the conversion of methyl acetoacetate and enantiomeric excess (ee) of the product, the reaction mixture was analyzed by gas chromatography and liquid chromatography. The gas chromatograph HP 5890 Series II was equipped with a FID detector and a HP-5 capillary column. Nitrogen was introduced as a carrier gas and the oven temperature was programmed from 45 to 200 °C with an initial duration of 15 min. The enantiomeric separation was achieved by Waters HPLC system equipped with a chiral column (Chiralpak AS, 0.46 cm × 25 cm, Daicel Industries) and an UV detector (λ = 210 nm). The enantiomeric excess (ee) was calculated from the equation:

$$\text{ee}\,(\%) = \frac{[\text{R-MHB}] - [\text{S-MHB}]}{[\text{R-MHB}] + [\text{S-MHB}]} \times 100$$

where [R-MHB] and [S-MHB] denote the concentrations of methyl (*R*)-3-hydroxybutyrate and methyl (*S*)-3-hydroxybutyrate, respectively.

2.3. Catalyst characterization

The specific BET surface areas, and pore size distributions were calculated from N_2 adsorption–desorption isotherms obtained on a constant volume adsorption apparatus (ASAP 2010C, Micrometrics) at −196 °C for samples degassed at 150 °C for 10 h.

The metal loading of prepared catalysts was determined by inductively coupled plasma-atomic emission spectroscopy (ICP-AES).

The phase of supported nickel was determined by powder X-ray diffraction (XRD) on a MAC Science diffractometer (Model M18XHF) operated at 40 kV and 200 mA with Cu Kα radiation of λ = 0.154 nm. The XRD patterns were obtained with a scanning range from 10° to 90° and a scanning rate of 4.0°/min. To probe the electronic state of nickel, X-ray photoelectron spectroscopy (XPS) experiment was carried out by using EscaLab 220-IXL with the source of Mg Kα ($h\nu$ = 1253.6 eV). The calcined samples were uniformly ground into fine powders together with gold powders and pressed to pellets. The binding energy of nickel was referenced to the peak of Au metal (84.0 eV for $4f_{7/2}$ core level). Then, the pellets of calcined samples without gold powders were reduced at 500 °C under H_2 stream, and analyzed by XPS. Temperature-programmed reduction (TPR) was performed with a reacting gas of 5% H_2 balanced with He. Temperature was ramped from 100 to 900 °C at a constant rate of 10 °C/min. The H_2O content of effluent was detected by a mass selective detector (HP MSD 5973).

The particle size and dispersion of nickel were estimated by CO chemisorption at room temperature, assuming hemispherical Ni particles and an adsorption stoichiometry (CO:surface Ni) of 1:2 [21,22,27]. The linear CO chemisorption and physisorption isotherms were obtained and the difference was extrapolated to zero pressure to calculate the amount of chemisorbed CO molecules. Transmission electron microscope (TEM) images were obtained on a Philips STEM CM 200 instrument operated at 200 kV. The samples were ultrasonically dispersed in ethanol in advance and loaded on a carbon-coated copper grid.

Table 1
Effects of supports and catalysts preparation methods on the texture of catalysts[a]

Supports	Supporting methods	Ni content (%)	BET area (m^2/g)	Mean particle size (nm)	Notation
Al_2O_3	Impregnation	40.5	79.6	29.8	Al_2O_3-Imp
Al_2O_3	Precipitation	38.9	101.4	26.0	Al_2O_3-Pre
SiO_2	Impregnation	39.8	104.2	20.4	SiO_2-Imp
SiO_2	Precipitation	38.5	336.8	9.2	SiO_2-Pre

[a] Catalysts were calcined at 500 °C for 5 h, and reduced at 500 °C for 2 h under hydrogen stream. The BET areas of pristine Al_2O_3 and SiO_2 were 160.0, and 204.2 m^2/g, respectively.

3. Results and discussion

3.1. Effects of supports and catalyst preparation methods

Table 1 shows the effects of supports and catalyst preparation methods on the texture and dispersion of catalysts. For all four catalysts, the nickel content was almost the same at 40 wt.% regardless of preparation methods and types of support. The BET areas of Al_2O_3-Imp, and Al_2O_3-Pre are 79.6 and 101.4 m^2/g, which are smaller than 160.0 m^2/g of the pristine Al_2O_3 support. SiO_2-Imp shows a BET area about 104.2 m^2/g which is ca. a half of SiO_2 support itself, but SiO_2-Pre has a BET area of 336.8 m^2/g which is larger than that of silica. The increased surface area suggests that the structure of SiO_2 has been completely changed upon nickel loading by precipitation, as discussed below. The pore size distributions of supports and calcined catalyst samples are listed in Fig. 1. The pristine Al_2O_3 support shows pore sizes around 3–4 nm and Al_2O_3-Pre, and Al_2O_3-Imp have pore size distribution peaks at 3 and 4 nm, respectively. The catalyst samples supported on Al_2O_3 have smaller pore volumes than the support before metal loading. It appears that the pore of Al_2O_3 support is partially blocked by nickel during sample preparation. SiO_2-Imp shows a similar trend; pore volume reduced from that of SiO_2 itself, especially for small pores of less than 30 nm. But SiO_2-Pre shows a completely different pore size distribution with a high peak around 3.5 nm. This completely reorganized pore structure may be responsible for the increased surface area of this sample relative to that of SiO_2 alone.

The mean particle size of nickel was measured by CO chemisorption. On Al_2O_3 support, larger nickel particles are formed probably due to the smaller specific surface areas. The impregnated samples show larger mean particle sizes of nickel than precipitated nickels on both supports. TEM images of four reduced samples are shown in Fig. 2. The nickel particle sizes of Al_2O_3-Imp, Al_2O_3-Pre, and SiO_2-Imp samples which are calculated by $\sum d_i n_i / \sum n_i$ agree with the values calculated from CO chemisorption in Table 1. But in the TEM image of SiO_2-Pre sample (Fig. 2(d)), nickel particles are highly dispersed on silica with the mean particle size of nickel around 5 nm, which is substantially smaller than the value of 9.2 nm obtained by CO chemisorption. We will discuss this phenomenon in Section 3.2.

3.2. Effects of preparation methods on the phase of nickel

The XRD patterns of calcined and reduced samples are listed in Fig. 3. In Fig. 3(a), four samples were calcined at 500 °C for 5 h. Al_2O_3-Imp, Al_2O_3-Pre, and SiO_2-Imp samples have a phase of crystalline nickel oxide (NiO) after the calcination step. But in the SiO_2-Pre sample, an amorphous phase of nickel silicate was detected while no nickel oxide phase was observed [1,28–31]. The phase of nickel silicate ($NiSiO_3$) was reported by Coenen [32], who

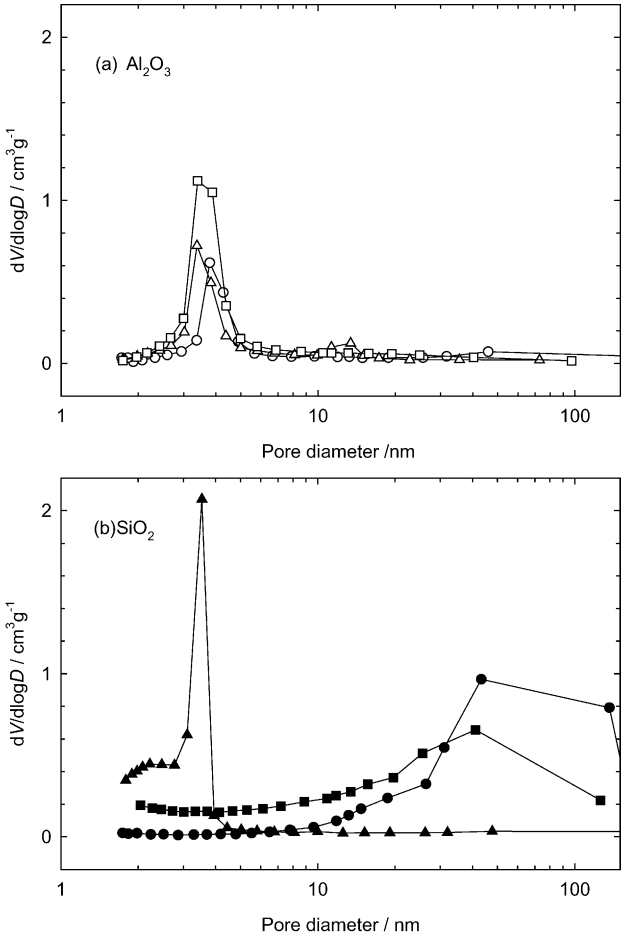

Fig. 1. Pore size distributions of calcined samples: (a) (□) Al_2O_3 support; (○) Al_2O_3-Imp; (△) Al_2O_3-Pre. (b) (■) SiO_2 support; (●) SiO_2-Imp; (▲) SiO_2-Pre samples.

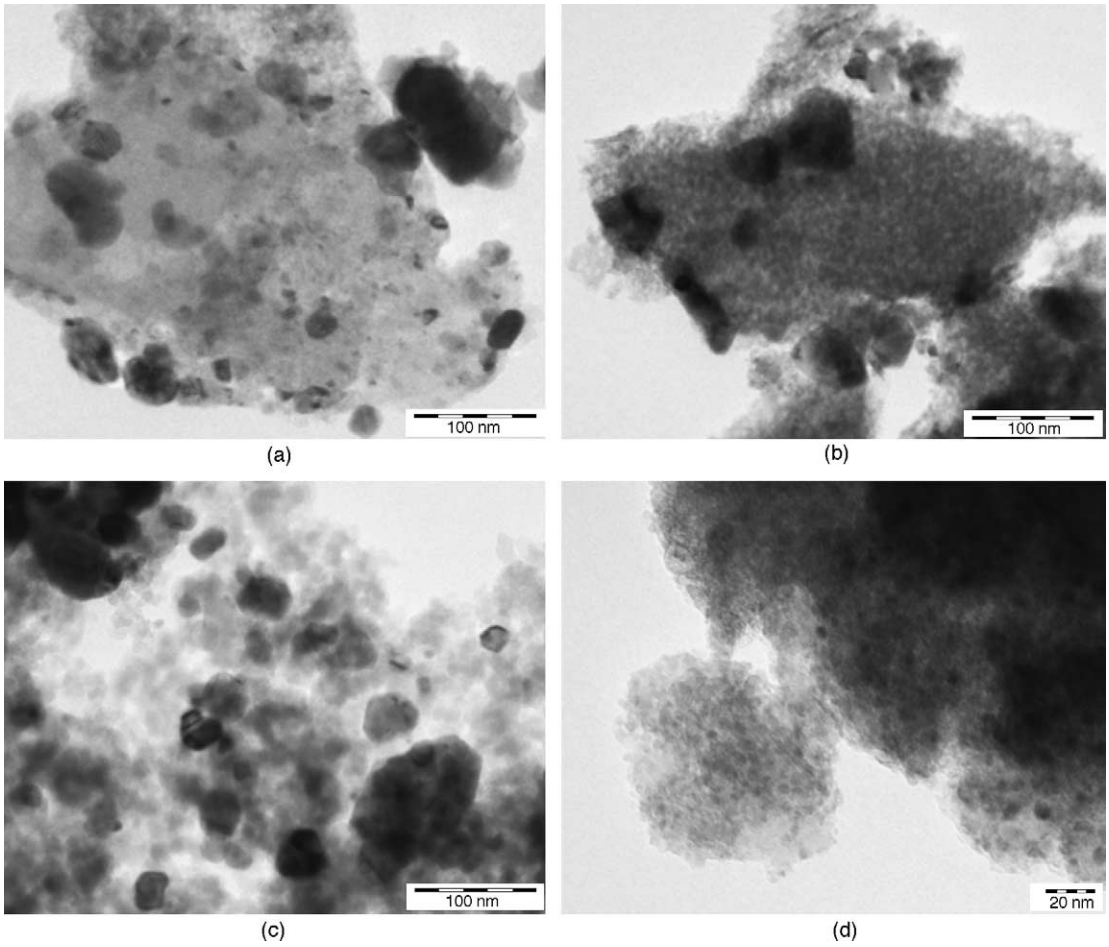

Fig. 2. TEM images of (a) Al_2O_3-Imp, (b) Al_2O_3-Pre, (c) SiO_2-Imp, and (d) SiO_2-Pre samples reduced at 500 °C.

prepared a silica-supported catalyst with a nickel content of about 25% by hydrolysis of urea in the precipitation reaction. This phase of nickel silicate was difficult to be reduced below 500 °C [1]. Fig. 3(b) shows the XRD patterns of samples reduced at 500 °C for 2 h under hydrogen stream. Like calcined samples, the crystalline phase of nickel metal was observed in the reduced Al_2O_3-Imp, Al_2O_3-Pre, and SiO_2-Imp samples, but not in the reduced SiO_2-Pre sample which is also amorphous. In reduced SiO_2-Pre, the metallic nickel phase is partially formed, but still the substantial portion of the nickel silicate phase remains unreduced. Thus, at the reduction temperature of 500 °C, the precipitated nickel on silica could not be completely reduced to nickel metal.

The reducibility of each calcined sample was determined by the temperature-programmed reduction (TPR), and the results are shown in Fig. 4. The majority of nickel in Al_2O_3-Pre, SiO_2-Imp, Al_2O_3-Imp, and SiO_2-Pre are reduced with the peak temperatures of 350, 400, 430, and 630 °C, respectively. Especially, the SiO_2-Pre sample shows a broad peak around 630 °C representing difficulty of reduction of nickel in this sample. Under the similar TPR conditions, the nickel precipitate obtained in the absence of silica showed a peak at 320 °C, while the phase of 2:1 phyllosilicate was reduced above 450–650 °C [28]. Thus, the reduction peaks observed at 350–450 °C for Al_2O_3-Imp, Al_2O_3-Pre, and SiO_2-Imp represent the reduction of supported nickel oxide with only a weak interaction with the support, while the higher reduction temperature above 600 °C for SiO_2-Pre represents the reduction of nickel silicate. In the reduction of Al_2O_3-Imp, a small second reduction peak at 580 °C could be due to the limited formation of $NiAl_2O_4$ phase [33] which comes from the dissolution of Al^{3+} ions during impregnation of the Al_2O_3 support with $Ni(NO_3)_2$ solution. In the SiO_2-Pre sample, the complete reduction of nickel was impossible at the reduction temperature of 500 °C. Overall, the nickel in the SiO_2-Pre sample has a very different local environment from that of other samples [34].

As shown in Table 1 and Fig. 2, the mean particle size of nickel from CO chemisorption was larger than that estimated from the TEM experiment at the SiO_2-Pre sample. The reason for this inconsistency is now obvious, i.e. the difficulty of reduction of nickel silicate. The nickel silicate of SiO_2-Pre was not completely reduced to nickel metal, and unreduced nickel remaining on the surface does not chemisorb CO, and thus the particle size of nickel metal based on CO chemisorption was overestimated.

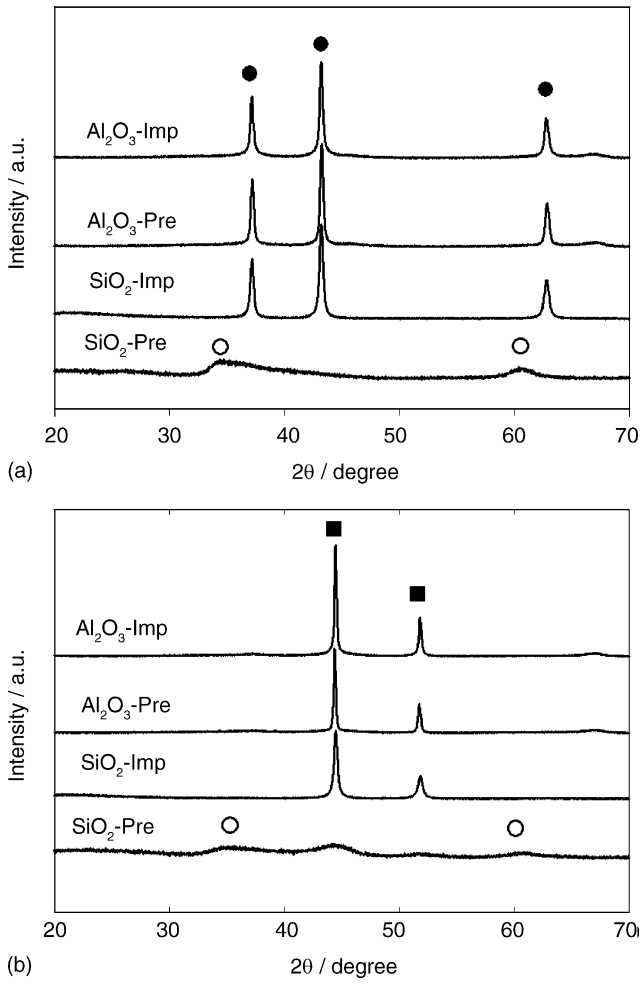

Fig. 3. XRD patterns of supported nickel after (a) calcination of 500 °C for 5 h, and (b) reduction at 500 °C for 2 h: (●) NiO; (◯) $NiSiO_3$; (■) Ni.

3.3. Effects of preparation method on the surface state of nickel

The surface state of nickel on supports was examined by X-ray photoelectron spectroscopy in both calcined (Fig. 5(a)) and reduced samples (Fig. 5(b)). Among four calcined samples, the SiO_2-Pre sample shows the state of nickel silicate ($NiSiO_3$) [35,36] as a single phase, and the other samples show the states of nickel oxide (NiO) [35] or nickel trioxide (Ni_2O_3) [37]. The SiO_2-Imp sample also shows a shoulder peak due to nickel silicate in a minor quantity. The nickel surface of calcined Al_2O_3-Imp and Al_2O_3-Pre are composed only of nickel oxides, NiO and Ni_2O_3. The phase of $NiAl_2O_4$ which is supposed to be present in the Al_2O_3-Imp sample due to the small TPR peak at 580 °C in Fig. 4 is not clearly seen in XPS experiments. This phase would have given a peak at 857 eV if present [38]. This peak appears to have been masked by strong peaks due to nickel oxides. Upon reduction of these samples, the surface phases of nickel oxide or nickel trioxide on Al_2O_3-Imp and Al_2O_3-Pre samples have been transformed to nickel metal. There are small portions

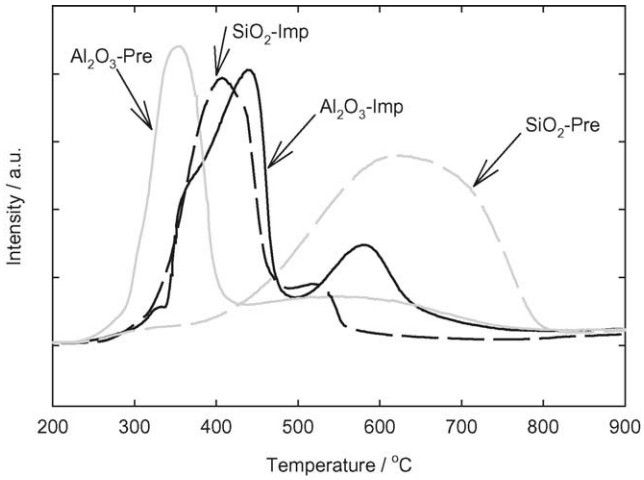

Fig. 4. H_2O release from the calcined samples by temperature-programmed reduction (TPR) of supported nickel oxides. Sample = 10.0 mg; ramping rate = 10 °C/min; flow rate (5% H_2 balanced with He) = 50 ml/min.

of unreduced nickel remaining, which might be due to the $NiAl_2O_4$ phase present as a minor phase in these samples before the reduction. In SiO_2-Imp, the majority of nickel oxide has been reduced to nickel metal, with a small portion remaining in nickel silicate. In SiO_2-Pre, a small portion of nickel silicate is reduced to nickel metal, but the majority of the surface state remains unreduced. So it could be concluded that the surface of nickel in Al_2O_3-Imp and Al_2O_3-Pre is well-crystallized nickel metal while in SiO_2-Imp and SiO_2-Pre, silicon from nickel silicate could contaminate the surface of nickel metal. Furthermore, the majority of nickel in SiO_2-Pre is nickel silicate, and even the reduced part of nickel surface would be contaminated by silicon.

3.4. Effects of preparation method on activity and enantio-selectivity of catalysts

In Table 2, the activity and enantio-selectivity of various catalysts are compared. It should be noted that these catalysts differ in preparation methods of supported nickel catalysts, but have been modified with (*R*,*R*)-tartaric acid and NaBr solution by the same procedure. The activity is represented in the time required to reach the given conversions of methyl acetoacetate. The catalyst prepared from SiO_2-Imp is more active than the others in asymmetric hydrogenation of methyl acetoacetate because of a better dispersion of nickel on silica with a higher surface area than aluminum oxide. However,

Table 2
Activity and enantio-selectivity of catalysts

Catalysts[a]	Conversion (%)	ee (%)
Al_2O_3-Imp	97.4 (10 h)	62.6
Al_2O_3-Pre	94.0 (23 h)	60.7
SiO_2-Imp	98.1 (3 h)	53.8
SiO_2-Pre	96.9 (300 h)	6.4

[a] The supported nickel catalysts were modified by (*R*,*R*)-tartaric acid and NaBr.

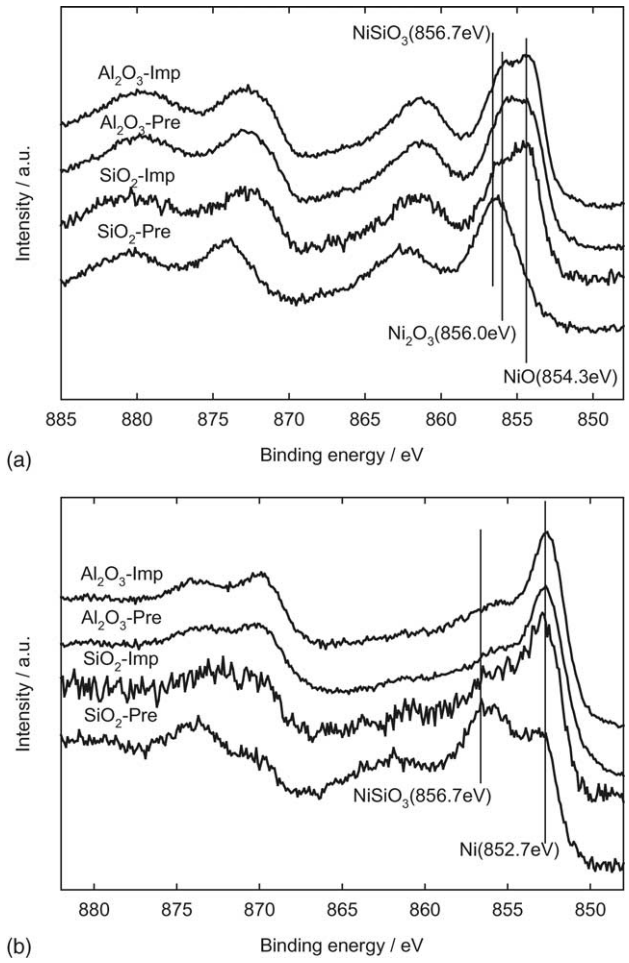

Fig. 5. XPS spectra of the Ni 2p region for calcined (a) and reduced (b) forms of supported nickel catalysts.

highly dispersed nickel on SiO_2-Pre shows a very slow reaction rate due to the unreduced nickel silicate on surface.

The ee's of product are also affected by the support type and preparation method. In order to exclude the effect of conversion on the enantio-selectivity, the selectivity is compared in Table 2 at similar conversions of 94.0–98.1%. Three catalysts SiO_2-Imp, Al_2O_3-Imp, and Al_2O_3-Pre have the enantio-selectivity above 50%. Following the well-established general trend, larger crystallite sizes of nickel give higher values of ee. But the catalyst prepared by the precipitation deposition method of nickel on silica (SiO_2-Pre) produces the product of an ee of 6.4%, nearly a racemic mixture. This is lower ee than the ee's of 20–30% for the catalysts of nickel loading about 11–15 wt.% [20,22,26,39], and 40–60% ee's for nickel loadings of 50 wt.% [18,40,41] prepared by the precipitation deposition of nickel on silica. This low ee of 6.4% obtained in the present study might be due to the use of fumed silica as a support. Fumed silica can be well mixed in aqueous nickel nitrate solution, so has more chance to form nickel silicate. Thus, this low enantio-selectivity of SiO_2-Pre catalyst is ascribed to the formation of nickel silicate. Nickel silicate of SiO_2-Pre catalyst is not completely reduced to nickel metal, and in addition, the reduced nickel surface should be contaminated by silicon, which may form many lattice defects on ensembles for enantio-selective sites. It was reported that the nickel surface with lattice defects decreased the enantio-selectivity of catalysts [14,42,43]. Thus the lattice defects on nickel surface of catalyst prepared from SiO_2-Pre may disrupt the arranged adsorption of tartaric acid, and decrease the enantio-selectivity of the catalyst. The catalyst prepared from SiO_2-Imp also contains a small portion of nickel silicate, and thus the enantio-selectivity of catalyst is less than that of Al_2O_3-Imp, and Al_2O_2-Pre.

4. Conclusions

Supported nickel catalysts were prepared with aluminum oxide and silica supports by the methods of impregnation and precipitation deposition and modified by (*R*,*R*)-tartaric acid and NaBr for the enantio-differentiating hydrogenation of methyl acetoacetate. All aluminum oxide-supported catalysts and the silica-supported catalyst prepared by impregnation gave high enantio-selectivities. However, the precipitated nickel on silica showed a low activity and a poor enantio-selectivity. The precipitated nickel on silica formed a very stable nickel silicate phase which was not fully reduced to nickel metal at 500 °C, and unreduced nickel silicate remained on the surface. Even the reduced nickel surface in this catalyst could be contaminated by the silicon. These effects disrupted the proper adsorption of tartaric acid on the nickel surface, and decreased the enantio-selectivity of catalyst.

Acknowledgements

We are grateful for the financial support provided by the Brain Korea 21 project of Ministry of Education in 2004, Korea.

References

[1] J.H. Bitter, M.K. van der Lee, A.G.T. Slotboom, A.J. van Dillen, K.P. de Jong, Catal. Lett. 89 (2003) 139–142.
[2] M.A. Ermakova, D.Y. Ermakov, Appl. Catal. A Gen. 245 (2003) 277–288.
[3] M.P. González-Marcos, J.I. Gutiérrez-Ortiz, C. González-Ortiz de Elguea, J.A. Delgado, J.R. González-Velasco, Appl. Catal. A Gen. 162 (1997) 269–280.
[4] T. Osawa, T. Harada, A. Tai, Catal. Today 37 (1997) 465–480.
[5] T. Osawa, T. Harada, O. Takayasu, Top. Catal. 13 (2000) 155–168.
[6] T. Osawa, S. Sakai, K. Deguchi, T. Harada, O. Takayasu, J. Mol. Catal. A Chem. 185 (2002) 65–69.
[7] P. Kukula, L. Čěrvený, J. Mol. Catal. A Chem. 185 (2002) 195–202.
[8] M. Studer, H.U. Blaser, C. Exner, Adv. Synth. Catal. 345 (2003) 45–65.
[9] T. Osawa, E. Mieno, T. Darada, O. Takayasu, J. Mol. Catal. A Chem. 200 (2003) 315–321.
[10] A. Tai, T. Harada, in: Y. Iwasawa (Ed.), Tailored Metal Catalysts, D. Reidel Publishing Company, Dordrecht, 1986, p. 265.

[11] G. Webb, in: G. Jannes, V. Dubois (Eds.), Chiral Reactions in Heterogeneous Catalysis, Plenum Press, New York, 1995, p. 61.
[12] R. Noyori, Asymmetric Catalysis in Organic Synthesis, Wiley, New York, 1993.
[13] A. Tai, T. Sugimura, in: D.E. De Vos, I.F.J. Vankelecom, P.A. Jacobs (Eds.), Chiral Catalyst Immobilization and Recycling, Wiley-VCH, Weinheim, 1998, p. 173.
[14] Y. Nitta, F. Sekine, T. Imanaka, S. Teranishi, Bull. Chem. Soc. Jpn. 54 (1981) 980–984.
[15] T. Osawa, S. Mita, A. Iwai, O. Takayasu, H. Hashiba, S. Hashimoto, T. Harada, I. Matsuura, J. Mol. Catal. A Chem. 157 (2000) 207–216.
[16] A. Wolfson, S. Geresh, M.V. Landau, M. Herskowitz, Appl. Catal. A Gen. 208 (2001) 91–98.
[17] S. Takahashi, T. Sato, N. Sodesawa, S. Nakamura, T. Tomiyama, S. Kosugi, Yoshida, J. Nanosci. Nanotechnol. 1 (2001) 169–176.
[18] T. Nitta, F. Sekine, T. Imanaka, S. Teranishi, J. Catal. 74 (1982) 382–392.
[19] Y. Nitta, O. Yamanishi, F. Sekine, T. Imanaka, S. Teraishi, J. Catal. 79 (1983) 475–480.
[20] L. Fu, H.H. Kung, W.M.H. Sachtler, J. Mol. Catal. 42 (1987) 29–36.
[21] M.A. Keane, G. Webb, J. Mol. Catal. 73 (1992) 91–95.
[22] M.A. Keane, Langmuir 13 (1997) 41–50.
[23] A. López-Martínez, M.A. Keane, J. Mol. Catal. A Chem. 153 (2000) 257–266.
[24] A. Hoek, W.M.H. Sachtler, J. Catal. 58 (1979) 276–286.
[25] L.J. Bostelaar, W.M.H. Sachtler, J. Mol. Catal. 27 (1984) 377–385.
[26] M.A. Keane, Catal. Lett. 19 (1993) 197–209.
[27] M.A. Keane, J. Chem. Soc., Faraday Trans. (1997) 93.
[28] P. Burattin, M. Che, C. Louis, J. Phys. Chem. B 101 (1997) 7060–7074.
[29] P. Burattin, M. Che, C. Louis, J. Phys. Chem. B 104 (2000) 10482–10489.
[30] P. Burattin, M. Che, C. Louis, J. Phys. Chem. B 103 (1999) 6171–6178.
[31] P. Burattin, M. Che, C. Louis, J. Phys. Chem. B 102 (1998) 2722–2732.
[32] J.W.E. Coenen, Appl. Catal. 54 (1989) 65–78.
[33] J.T. Richardson, M.V. Twigg, Appl. Catal. A Gen. 167 (1998) 57–64.
[34] R. Tomiyama, S. Takahshi, T. Sato, S. Sodesawa, Yoshida, Appl. Catal. A Gen. 241 (2003) 349–361.
[35] P. Lorenz, J. Finster, G. Wendt, J. Electron. Spectrosc. Relat. Phenom. 16 (1979) 267–276.
[36] R.B. Shalvoy, R.J. Reucroft, B.H. Davis, J. Catal. 56 (1979) 336–348.
[37] L. Salvatl Jr., L.E. Makovsky, J.M. Stencel, F.R. Brown, D.M. Hercules, J. Phys. Chem. 85 (1981) 3700–3707.
[38] S. Kasztelan, J. Grimblot, J.P. Bonnelle, E. Payew, H. Toulhoat, Y. Jacquin, Appl. Catal. 7 (1983) 91–112.
[39] M.A. Keane, G. Webb, J. Catal. 136 (1992) 1–15.
[40] Y. Nitta, T. Imanaka, S. Teranishi, J. Catal. 96 (1985) 429–438.
[41] Y. Nitta, T. Utsumi, T. Imanaka, S. Teranishi, J. Catal. 101 (1986) 376–388.
[42] J. Masson, P. Cividino, J. Court, J. Mol. Catal. A Chem. 111 (1996) 289–295.
[43] T. Osawa, Y. Amaya, T. Harada, O. Takayasu, J. Mol. Catal. A Chem. 211 (2004) 93–96.